ACS Chemical Neuroscience

Research Article

pubs.acs.org/chemneuro

APP+, a Fluorescent Analogue of the Neurotoxin MPP+, Is a Marker of Catecholamine Neurons in Brain Tissue, but Not a Fluorescent False Neurotransmitter

Richard J. Karpowicz, Jr.,[†] Matthew Dunn,[†] David Sulzer,*[,‡,§] and Dalibor Sames*[,†]

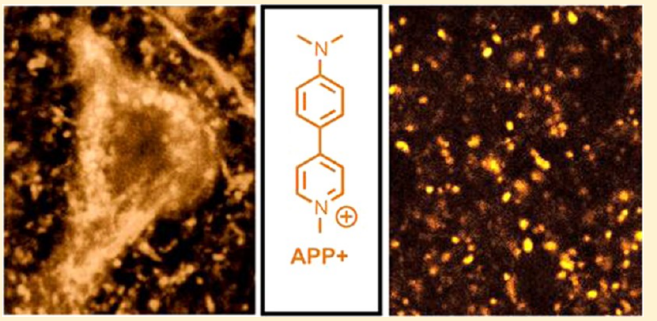
[†]Department of Chemistry, Columbia University, 3000 Broadway, New York New York 10027, United States

[‡]Departments of Neurology, Psychiatry and Pharmacology, Columbia University Medical Center, New York, New York 10032, United States

[§]Department of Neuroscience, New York Psychiatric Institute, New York, New York 10032, United States

Supporting Information

ABSTRACT: We have previously introduced fluorescent false neurotransmitters (FFNs) as optical reporters that enable visualization of individual dopaminergic presynaptic terminals and their activity in the brain. In this context, we examined the fluorescent pyridinium dye 4-(4-dimethylamino)phenyl-1-methylpyridinium (APP+), a fluorescent analogue of the dopaminergic neurotoxin MPP+, in acute mouse brain tissue. APP+ is a substrate for the dopamine transporter (DAT), norepinephrine transporter (NET), and serotonin transporter (SERT), and as such represented a candidate for the development of new FFN probes. Here we report that APP+ labels cell bodies of catecholaminergic neurons in the midbrain in a DAT- and NET-dependent manner, as well as fine dopaminergic axonal processes in the dorsal striatum. APP+ destaining from presynaptic terminals in the dorsal striatum was also examined under the conditions inducing depolarization and exocytotic neurotransmitter release. Application of a high concentration of KCl led to a small but significant degree of destaining (approximately 15% compared to control), which stands in contrast to a nearly complete destaining of the new generation FFN agent, FFN102. Electrical stimulation of brain slices at 10 Hz afforded no significant change in the APP+ signal. These results indicate that the majority of the APP+ signal in axonal processes originates from labeled organelles including mitochondria, whereas only a minor component of the APP+ signal represents the releasable synaptic vesicular pool. These results indicate that APP+ may serve as a useful probe for identifying catecholaminergic innervations in the brain, although it is a poor candidate for the development of FFNs.



KEYWORDS: *APP+, neuronal imaging agent, fluorescent false neurotransmitters, catecholamine neurons, two-photon microscopy, acute mouse brain slice*

Chemical labels and stains, together with technological advancements in microscope design, have played a crucial role in the development of modern neuroscience by revealing morphology of neurons, their discrete nature, organization and layering of neuronal cell bodies in the tissue, and the structures of fine axonal and dendritic processes.[1] Due to the higher detection sensitivity of fluorescence microscopy compared to light microscopy, development of fluorescent dyes as selective labels represents an active area of research. For example, fluorescent compounds that enable selective labeling of specific cell types[2,3] and organelles[4] are widely used research tools. In addition to fluorescent labeling of specific subcellular and molecular structures, functional fluorescent probes and sensors were developed that enable imaging of important physiological parameters or processes such as intracellular calcium concentrations,[5,6] membrane potential,[7] and exocytosis/endocytosis,[8] with high spatial and temporal resolution. However, despite the central importance of neurotransmission at the chemical synapse for brain function, fluorescence imaging of neurotransmitter release at individual synapses in the brain has been difficult.[9]

To address this challenge, we have introduced the concept of fluorescent false neurotransmitters (FFNs) as optical reporters of neurotransmitters. FFNs enable labeling of presynaptic terminals and visualization of neurotransmitter release at individual synapses in the brain as demonstrated in the context of dopamine (DA) neurons.[10,11]

Special Issue: Monitoring Molecules in Neuroscience

Received: February 5, 2013
Accepted: April 21, 2013

ACS Publications © XXXX American Chemical Society

dx.doi.org/10.1021/cn400038u | ACS Chem. Neurosci. XXXX, XXX, XXX–XXX

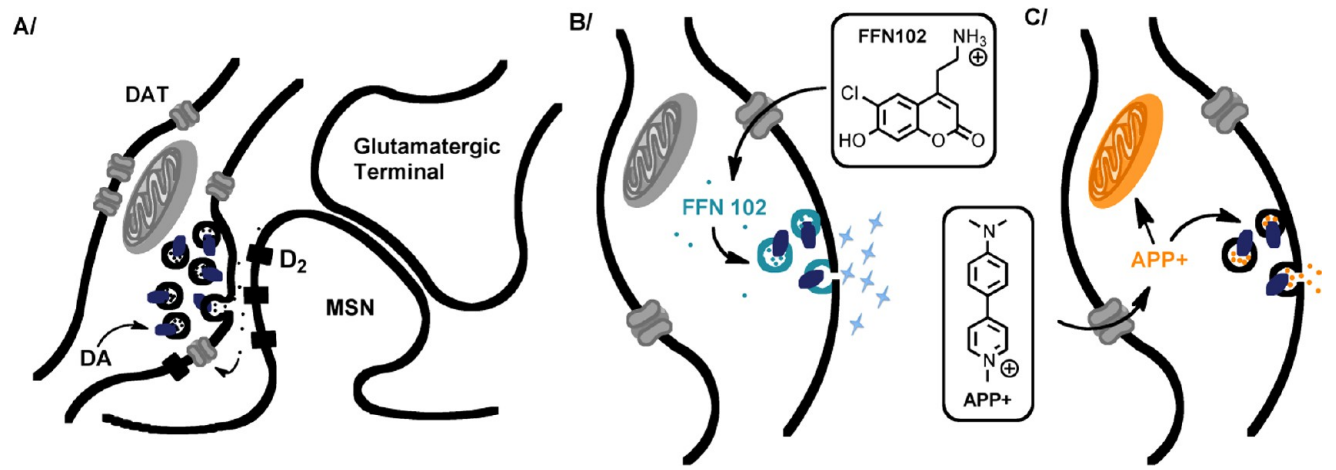


Figure 1. Overview of a representative dopaminergic synapse and labeling by FFNs and APP+. (A) Dopamine is synthesized in the DA neuron and packaged into synaptic vesicles by the action of VMAT2 (blue ovals). Upon arrival of an action potential, DA is released via exocytosis into the synaptic cleft and extrasynaptic space where it interacts with pre- and postsynaptic dopamine receptors, and is transported in large part back into the presynaptic neuron via DAT. MSN = medium spiny neuron, D_2 = dopamine receptor D_2. (B) FFNs such as FFN102 are actively transported into dopaminergic axonal structures and stain both the cytosol and the synaptic vesicles. (C) Analogously, according to the proposed model, APP+ is transported via the same plasma membrane transporters, although APP+ then labels mitochondria, driven by the electrochemical potential across the mitochondrial inner membrane, as well as synaptic vesicles via VMAT2. The polar environment inside the cytosol and synaptic vesicle lumen likely leads to significant quenching of APP+ fluorescence. The vesicular signal is overwhelmed by the fluorescence from mitochondria, resulting in a nonreleasable fluorescent signal.

In the central nervous system, dopamine modulates the strength of both excitatory (glutamate) and inhibitory (GABA) synapses via activation of the corresponding receptors. The dopaminergic system plays important roles in sensory-motor coordination, reward and motivation processes, and attention modulation.[12] Endogenous DA is synthesized in DA neurons and sequestered by vesicular monoamine transporter 2 (VMAT2) into synaptic vesicles (Figure 1A). Upon exocytosis, DA is released to the synapse and the extrasynaptic space where it activates dopamine receptors.[13] The DA signal is primarily terminated by the plasma membrane dopamine transporter (DAT), which transports DA into the cytosol.[14] The recycled DA is subsequently accumulated into synaptic vesicles as a substrate of VMAT2, or metabolized. We recently introduced a new generation of pH-responsive FFN probes, represented by the compound FFN102 (Figure 1B). FFN102 mimics dopamine in several key aspects: as a dual DAT and VMAT2 substrate, FFN102 labels dopamine neuronal bodies and presynaptic terminals with high selectivity and is released upon exocytosis, thus enabling imaging of individual presynaptic varicosities and their activity in acute mouse brain slice preparations. However, unlike DA, FFN102 has negligible affinity for a panoply of receptor targets.

As a part of the FFN research program, we became interested in fluorescent analogues of the neurotoxin 4-phenyl-*N*-methylpyridinium (MPP+, Figure 2). MPP+ is a known substrate for DAT,[15,16] the norepinephrine transporter (NET),[17] and the serotonin transporter (SERT),[18] as well as for VMAT2.[19−21] Selective accumulation of MPP+ in catecholamine neurons and inhibition of mitochondrial respiration was proposed as the mechanism for the toxic effects in these cells, with the most extensive degeneration occurring in the nigrostriatal dopaminergic system.[15,22] MPP+ was also shown to load dopaminergic presynaptic terminals in rat striatum and to be released upon potassium chloride-induced exocytosis.[23] Further, the fluorescent analogue of MPP+, 4-(4-dimethylaminostyryl)-*N*-methylpyridinium (ASP+), has been shown to act as a substrate of plasma membrane monoamine neurotransmitter transporters, demonstrating that activity of these transporters can be monitored using fluorescent substrates.[24−26] Based on these reports and those showing vesicularization of MPP+, we hypothesized that a small fluorescent analogue of MPP+ could potentially function as a FFN. We chose to examine an analogue containing the strongly electron-donating dimethylamino group, 4-(4-dimethylamino)-phenyl-1-methylpyridinium (APP+, Figure 2). APP+ was originally reported as an antibacterial dye.[27] It was subsequently shown to exhibit negative solvatochromic photophysical properties;[28] its absorbance maximum is blueshifted in polar environments. Additionally, it is fluorescent in hydrophobic media and quenched in aqueous environments.[29] This property was ascribed to light emission quenching via a twisted intramolecular charge transfer (TICT) mechanism, enabled by the perpendicular conformation of the two arene rings. These photophysical properties are shared by the other members of the pyridinium class of dyes, including ASP+,[24] 2-(4-dimethylaminostyryl)-*N*-methylpyridinium (DASPMI),[30] and the FM dyes.[31] Recently, APP+ was also shown to be a substrate for DAT, NET, and SERT, providing a reporter substrate for this important group of plasma membrane transporters and enabling cell-based assays for examining their function and inhibition.[32,33] Additionally, the commercially available Neurotransmitter Transporter Uptake Assay Kit (NTUA; Molecular Devices) has been used by several laboratories,[34−36] and although the exact nature of the fluorescent compound is not provided by the vendor, it has been suggested to be a pyridinium dye derivative.[36] However, the potential of APP+ to serve as a fluorescent label for monoamine neurons in the brain or as an FFN has not been previously reported.

In this report, we examine APP+ in acute mouse brain tissue with respect to selectivity of labeling of dopamine and norepinephrine neuronal cell bodies in the midbrain, labeling of dopaminergic axonal processes and presynaptic nerve

dx.doi.org/10.1021/cn400038u | ACS Chem. Neurosci. XXXX, XXX, XXX−XXX

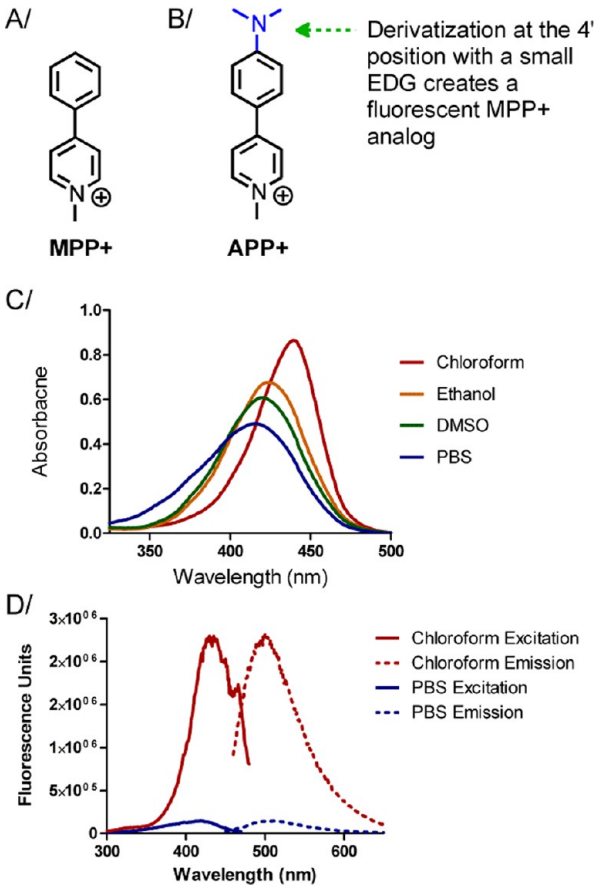


Figure 2. Structure and photophysical properties of APP+. (A) Structure of the monoaminergic neurotoxin MPP+, which served as a lead for these studies. (B) Addition of a strongly electron-donating group (EDG) to the 4′ position of MPP+ generates APP+, a small, fluorescent analogue. (C) UV−vis spectra of APP+ (20 μM) in different solvents illustrating the blue-shift of the absorbance maximum with increasing solvent polarity, characteristic of pyridiniums (λ_{max}PBS = 416 nm, λ_{max}DMSO = 419 nm, λ_{max}ethanol = 424 nm, $\lambda_{max}CHCl_3$ = 439 nm). (D) Emission and excitation profiles of APP+ (2 μM) in phosphate buffered saline (PBS), pH = 7.4 (λ_{ex}PBS = 417 nm, λ_{em}PBS = 501 nm), and chloroform ($\lambda_{ex}CHCl_3$ = 436 nm, $\lambda_{em}CHCl_3$ = 506 nm), illustrating the strong solvent effects to which APP+ is subject. Spectra were measured at the corresponding emission/excitation maxima for APP+ in the respective solutions. Importantly, APP+ is approximately 10 times more fluorescent in nonpolar environments than in aqueous buffer.

elements in the dorsal striatum, and release of APP+ from dopaminergic release sites. A simple mechanistic model is provided to account for the observed labeling and release properties.

RESULTS

Photophysical Characterization of APP+ Iodide. APP+ iodide was synthesized via a two-step sequence as described in the Supporting Information (Scheme S1). APP+ is an organic cationic dye that displays solvatochromic photophysical properties: its absorption is blue-shifted in polar media (Figure 2C); it is highly fluorescent in nonpolar solvents, while its fluorescence is largely quenched in polar solvents, consistent with previous reports.[28,29] Specifically, we found that APP+ was approximately 10 times more fluorescent in chloroform than in aqueous PBS buffer (Figure 2D). Excitation maxima were found to be 417 nm in PBS and 436 nm chloroform. Emission maxima are 502 nm in PBS and 506 in chloroform when excited at the corresponding excitation maxima.

APP+ Labels Mitochondria in hDAT-Transfected EM4 Cells. We set out to confirm the intracellular localization of APP+ using hDAT-transfected EM4 cells (Figure 3). Both

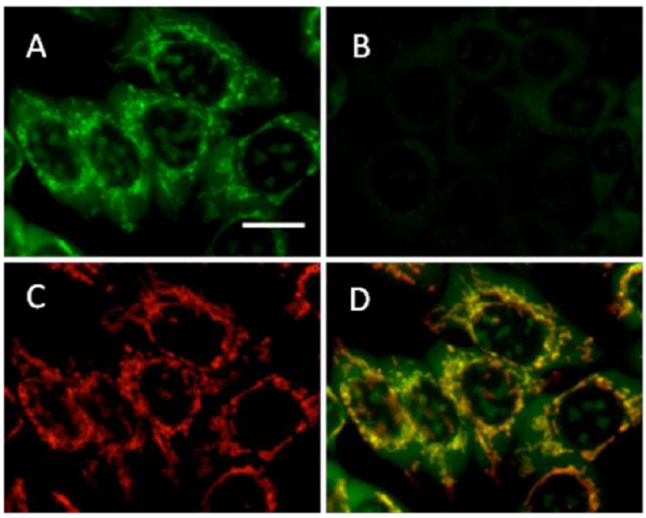


Figure 3. APP+ becomes localized in mitochondria of EM4 cells expressing hDAT. Shown are epifluorescence microscopy images of APP+ (2 μM, 10 min incubation) in (A) hDAT-transfected EM4 cells and (B) empty vector-transfected EM4 cells. (C) hDAT-transfected EM4 cells were also coincubated with Mitotracker Deep Red (20 nM, 10 min). (D) Overlay of APP+ and Mitotracker images shows strong colocalization, indicating mitochondrial concentration of APP+. Scale bar = 15 μm.

hDAT-transfected and empty vector-transfected EM4 cells were coexposed for 10 min with Mitotracker Deep Red (20 nM) and APP+ (2 μM). Each probe was imaged separately by using the appropriate optical filters with no cross-channel signal contamination (see Methods). Both cell types were similarly stained by the Mitotracker dye (Figure 3C), while APP+ accumulated rapidly in hDAT-transfected EM4 cells. The empty-vector transfected EM4 cells afforded no significant uptake of APP+ under the same conditions (Figure 3B). A high degree of colocalization of APP+ and Mitotracker in hDAT-transfected cells (Figure 3D) confirms that APP+ labels mitochondria in these cells, which is consistent with a previous report using a SERT-expressing cell line,[33] and is ascribed to the permanent positive charge on APP+.[22] The quenched fluorescence in aqueous growth media is advantageous for cell culture assays, as continuous measurement or imaging is possible in the presence of APP+ dye with no need for washing or additional quenching agents.

APP+ Labels Catecholamine Neurons in the Midbrain. Previous studies investigating APP+ uptake by cells have been limited to cultured cells transfected with plasma membrane monoamine transporters,[32,33] cultured cells endogenously expressing SERT,[37] or platelets and lymphocytes.[38] We therefore examined labeling characteristics of APP+ in acute mouse brain slices containing the midbrain region. The labeling selectivity was determined by colocalization of the APP+ and GFP signals in brain tissue obtained from mice expressing GFP under the control of tyrosine hydroxylase (TH) promoter (TH-GFP mice),[39] via two-photon microscopy (Figure 4). For

dx.doi.org/10.1021/cn400038u | ACS Chem. Neurosci. XXXX, XXX, XXX−XXX

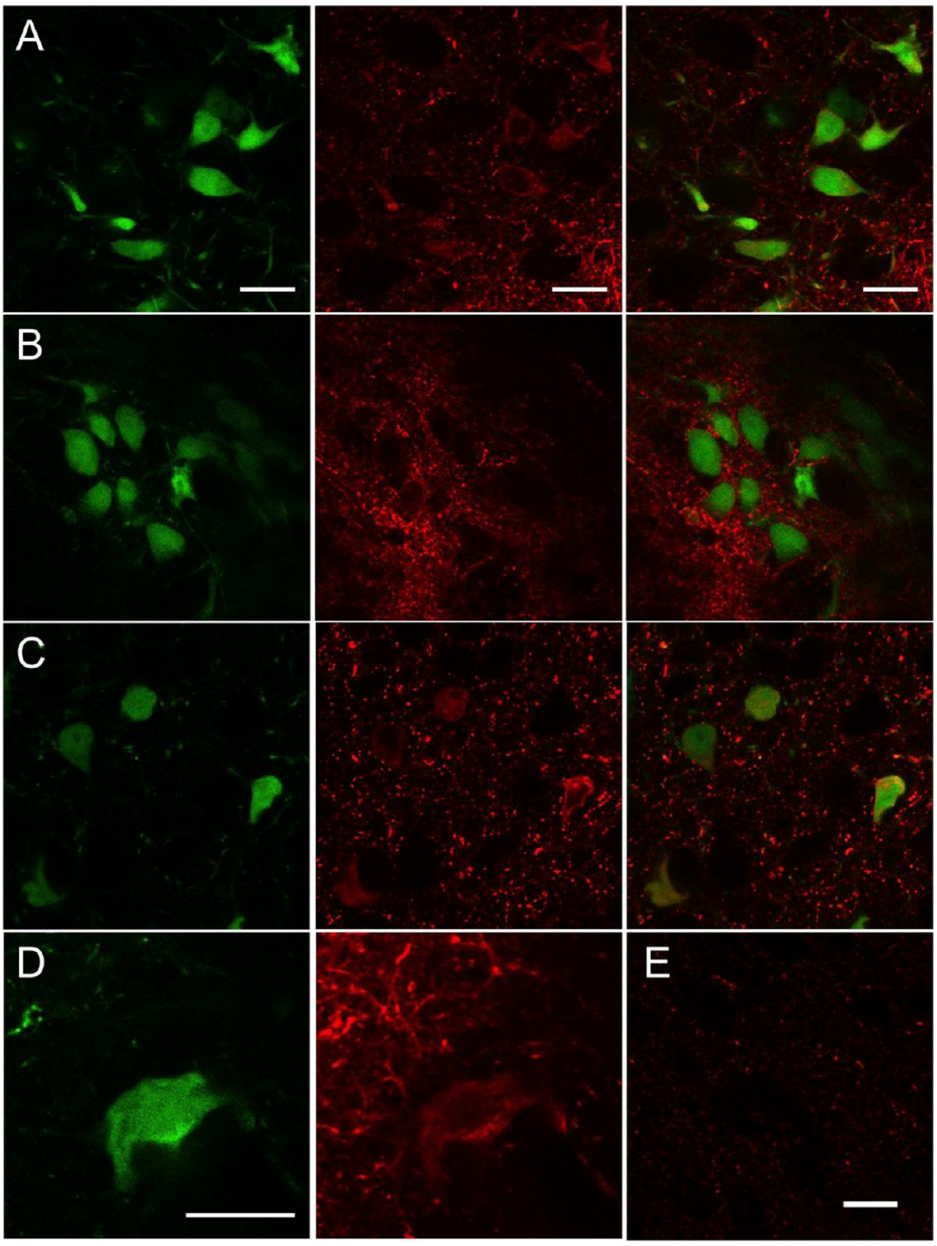


Figure 4. APP+ labels catecholaminergic neuronal cell bodies in acute mouse midbrain slices. TH-positive cell bodies (TH-GFP in green) in the (A) DAT-expressing ventral tegmental area and substantia nigra (VTA/SN), and (C) NET-expressing locus coeruleus (LC) accumulate APP+ (in red) in a selective manner relative to other cell bodies (black holes) after perfusion of APP+ (500 nM) for 30 min. (B) Accumulation of APP+ into cell bodies in the SN/VTA can be substantially inhibited if the slice is pretreated with a DAT inhibitor (nomifensine, 1 μM; scale bar = 20 μm). (D) A closer view of an APP+ labeled cell body from SN/VTA illustrates a perinuclear, punctate staining pattern similar to what is seen in hDAT-transfected EM4 cells, suggesting mitochondrial staining (TH-GFP in green, APP+ in red; scale bar = 20 μm). (E) No staining of cell bodies was observed in the primary visual cortex of the same slice (scale bar = 20 μm).

dopamine cell bodies, we examined the substantia nigra pars compacta region (SN) and the ventral tegmental area (VTA), the anatomical areas where the neuronal cell bodies of the nigrostriatal and mesolimbic dopaminergic systems, respectively, reside. Acute midbrain slices from TH-GFP transgenic mice were perfused for 30 min with oxygenated ACSF containing 500 nM of APP+, followed by washing for 10 min with oxygenated ACSF. Staining patterns and colocalization were determined by imaging individual slices sequentially at the excitation and emission wavelengths for APP+ and GFP (APP+: λ_{ex} = 800 nm, λ_{em} = 435−485 nm; GFP: λ_{ex} = 950 nm, λ_{em} = 500−550 nm). Excitation and emission wavelengths were chosen to minimize signal crosstalk between APP+ and GFP channels (Supporting Information Figure S1). Labeled cell bodies were defined as areas with mean fluorescence intensity greater than two standard deviations above background signal, with size and shape consistent with morphological parameters of dopamine neuronal soma. Colocalization was determined by assessing the number of cell bodies in each region where GFP signal and APP+ signal were both present at least two standard deviations above their respective backgrounds.

Every cell body labeled by APP+ in these regions was found to contain the GFP signal, while 76% of TH-GFP positive cells in SN/VTA contained the APP+ signal (84/110 cells, n = 6,

dx.doi.org/10.1021/cn400038u | ACS Chem. Neurosci. XXXX, XXX, XXX−XXX

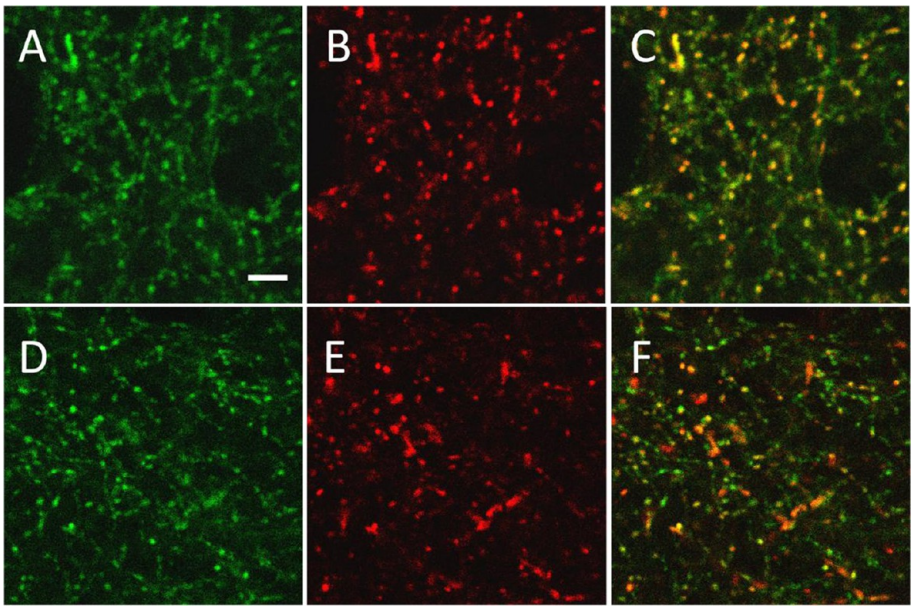


Figure 5. APP+ colocalizes with dopaminergic markers in the dorsal striatum. (A) Signal from GFP expressed under control of the TH promotor. (B) 100 nM APP+ perfusion for 15 min creates a punctate staining pattern in dorsal striatal acute slices. (C) APP+ colocalizes well with TH-GFP (83.4 ± 6.9%, mean ± SD, n = 3). Because of a small amount of crosstalk between APP+ and GFP channels, we confirmed dopaminergic labeling with another marker, FFN102, which has previously been shown to label dopaminergic terminals in the dorsal striatum. (D) FFN102 staining in the same frame. (E) APP+ staining when loaded under the same conditions as above in the presence of FFN102. (F) Overlay of the two channels shows good colocalization of puncta (74.1 ± 6.9%, mean ± SD, n = 3), confirming APP+ as a marker for dopaminergic innervations in the dorsal striatum. Scale bar = 5 μm.

Figure 4A). Further, the DA neuronal cell body labeling was greatly reduced by treatment of the slice with the DAT inhibitor nomifensine[40] (7%, 3/43 cells, n = 3, Figure 4B), confirming that APP+ uptake by DA neuronal soma is DAT dependent. The higher magnification image shows a heterogeneous perinuclear staining (Figure 4D) similar to that observed in hDAT-EM4 cells (Figure 3), suggesting mitochondrial staining. These results indicate that APP+ selectively labels DA neuronal cell bodies versus other neurons in the area, which appear as dark unstained regions (Figure 4A).

To obtain the level of soma labeling specified above, incubation of the slice with 500 nM APP+ for 30 min (Methods) was required. Under these conditions, a high level of punctate staining was observed, which was not inhibited by nomifensine in SN/VTA (Figure 4A,B), and was also present in brain areas outside of SN/VTA (Figure 4E). These results indicate that the majority of the background staining is not related to DA neuronal structures such as the dendrites.

We also investigated labeling of noradrenergic neurons in the locus coeruleus (LC) where the majority of noradrenergic cell bodies reside (Figure 4C). APP+ selectively labeled these neurons; all APP+ labeled cells contained the GFP signal and 59% of TH-GFP positive cells in LC were also labeled with APP+ (74/126 GFP positive cells, n = 3). We found that for analysis of APP+ uptake by noradrenergic neurons in LC, young mice (<30 days postnatal) were required, as the staining was dim and inconsistent in older mice (data not shown). This finding is consistent with reported down-regulation of NET protein expression in cell bodies of noradrenergic neurons in the LC of older mammals, including mice.[41,42] As in the SN/VTA region, APP+ provides a high level of punctate background staining in LC.

Our studies demonstrate that APP+ labels catecholamine neurons in the indicated brain areas in a DAT/NET dependent manner. Despite the fair degree of unidentified fluorescent puncta, the catecholamine neuronal cell bodies could be readily identified in acute unfixed brain slices by simple perfusion of the tissue with the APP+ dye.

APP+ Labels Dopaminergic Axonal Processes in Dorsal Striatum. The dorsal striatum is heavily innervated by the dopamine neurons originating in SN (see above). Among other functions, DA in the dorsal striatum modulates excitatory inputs from the cortex and other brain areas and plays crucial roles in sensory-motor coordination and habit formation.[43] A coronal slice comprising the dorsal striatum was loaded with APP+ using the experimental conditions described above, except that a lower concentration of APP+ (100 nM) for only 15 min was sufficient to provide bright, punctate staining (Figure 5A). The overall pattern of APP+ staining is similar to that of GFP in TH-GFP mice. Quantitative comparison showed a good degree of colocalization: 83.4 ± 6.9% (mean ± SD, n = 3) of APP+ puncta contained the GFP signal (Figure 5A–C). We observed a small degree of APP+ signal contamination in the GFP channel, enough for the brightest 10.1 ± 5.7% of the APP+ labeled puncta to be picked up in the GFP channel of GFP negative brain slices (mean ± SD, n = 3; see Supporting Information Figure S2 for control images). To provide another quantitative colocalization measure in absence of significant signal crosstalk, we also examined colocalization of APP+ and FFN102 in wild type mice (see Supporting Information Figure S3 for control images). As discussed above, FFN102 is to date the most selective FFN probe for dopamine neurons, featuring strong DAT dependence and ~90% colocalization with TH-GFP signal in dorsal striatum, and thus may serve as a reliable reference signal.[11] We found that 74.1 ± 6.9% (mean ± SD, n = 3) of APP+ puncta were FFN102 positive (Figure 5D–F). These results indicate that APP+ labels fine axonal processes of

dx.doi.org/10.1021/cn400038u | ACS Chem. Neurosci. XXXX, XXX, XXX–XXX

dopamine neurons in the dorsal striatum with selectivity > 70% as defined by colocalization to two reference signals.

We next examined whether the selectivity of APP+ for DA axonal processes was DAT dependent. Preincubation of slices with nomifensine (1 μM, 15 min), followed by a 15 min coincubation of nomifensine (1 μM) and APP+ (100 nM) under continuous perfusion in oxygenated ACSF reduced the number of APP+ labeled puncta per image by 2.3-fold, from 147.8 ± 1.4 to 61.4 ± 10.0 (mean ± SD, n = 3) (Figure 6C).

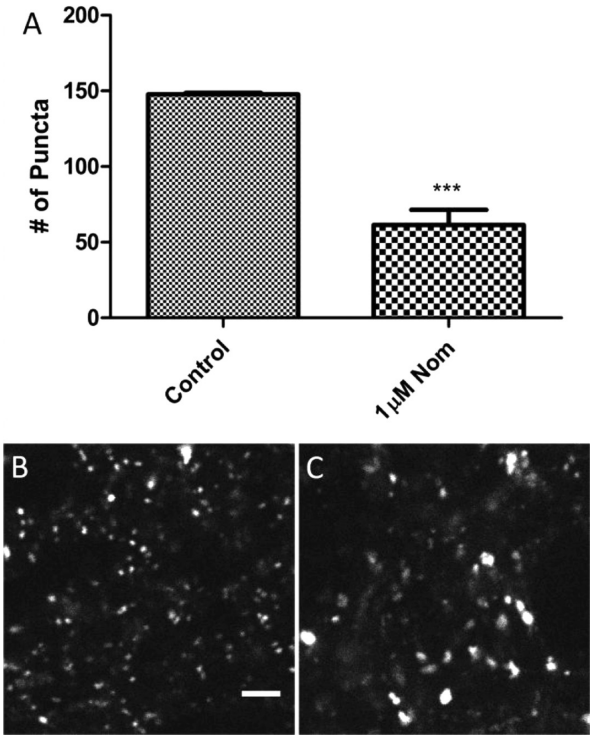


Figure 6. APP+ uptake into dorsal striatum is inhibited with the DAT blocker nomifensine. (A) Representative image of APP+ staining in mouse dorsal striatum (100 nM, 15 min perfusion). (B) Pretreatment with nomifensine (1 μM, 15 min) followed by cotreatment with APP+ (100 nM, 15 min perfusion) significantly reduces the number of stained puncta while changing the appearance of remaining structures. (C) Nomifensine significantly reduces the mean number of puncta per frame from 147.8 ± 1.4 to 61.4 ± 10.0 (mean ± SD, significance determined by t test, p < 0.001, n = 3). Scale bar = 5 μm.

Further, the staining pattern of the dorsal striatum was dramatically different under the DAT-inhibition conditions compared to that of control slices; the remaining puncta were more heterogeneous in size and brightness, owing to formation of large bright puncta (Figure 6A,B). These findings suggest that additional transporter systems are present in the dorsal striatum that may facilitate APP+ uptake when DAT is inhibited (see Discussion below).

Partial Destaining of APP+ Induced by KCl. Neuronal depolarization and subsequent exocytotic release of neurotransmitters can be induced in vitro by high potassium concentrations. We have previously shown that FFN102-loaded presynaptic terminals in dorsal striatum were completely destained through the action of 40 mM KCl.[11] With APP+, however, we found that KCl only partially destained terminal fields compared to ACSF-treated control (Figure 7). Analysis was accomplished by measuring mean fluorescence intensity of a field of background-subtracted puncta, before and during KCl

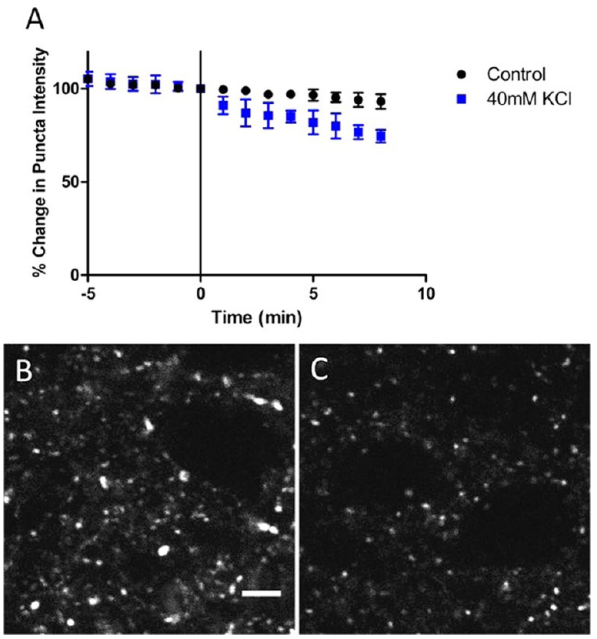


Figure 7. Treatment of APP+ loaded dopaminergic axonal structures with KCl leads to a small but significant degree of destaining. (A) Dorsal striatal slices were loaded with APP+ (100 nM) and treated with a KCl (40 mM) to induce depolarization and exocytosis. Images were collected every 60 s. APP+ destaining was greatest at 8 min after application of KCl. Release was statistically significant after 1 min of KCl treatment compared to a control imaged without KCl (t test, p < 0.05 from t = 1−3 min, p < 0.01 from t = 4−8 min). (B) Representative image of APP+ signal at t = 0 min. (C) Representative image of APP+ signal at t = 8 min. Scale bar = 5 μm.

treatment, and comparing the results to those obtained with a control imaged without KCl treatment. It is important to note that individual puncta could not be tracked throughout the course of this experiment due to the high degree of slice movement upon KCl stimulation (presumably owing to widespread and rapid depolarization and exocytosis). We found that the mean APP+ signal collected from all labeled structures is reduced by 15.3 ± 2.5% after 8 min of KCl treatment (mean ± SD, n = 3; t test, p < 0.05 for t = 1−3 min, p < 0.01 for t = 4−8 min). These results show that, under the conditions of prolonged depolarization and exocytosis, APP+ is released from presynaptic terminals in a small but significant manner. This is consistent with previously reported release of MPP+ under similar depolarization conditions.[23] We were not able to observe the released APP+ in the extracellular space with two-photon microscopy, most likely due to quenching of APP+ fluorescence in aqueous media (Figure 2).

No Significant Destaining of APP+ is Achieved by Local Electrical Stimulation in the Dorsal Striatum. Local electrical stimulation induces depolarization and exocytosis by application of electrical current via a bipolar electrode and enables the control over the frequency and number of pulses applied to the brain region of interest. Electrical stimulation leads to far less slice deformation and movement in comparison to KCl perfusion and thus allows for measuring release kinetics of individual puncta. To study the effects of electrical stimulation on APP+ in the dorsal striatum, we employed a method used routinely in our laboratories for determining the kinetics of electrically stimulated FFN release (see Methods), which involves imaging z-stacks at 15 s intervals. Under these

dx.doi.org/10.1021/cn400038u | ACS Chem. Neurosci. XXXX, XXX, XXX−XXX

conditions, it became apparent that photobleaching would obscure exocytotic destaining of puncta, as 73 ± 25% of APP+ signal was lost after application of the imaging sequence (controlled to slices imaged only at the start and end of the experiment; mean ± SD). We thus sampled a greater number of *z*-sections throughout the experiment while exciting each *z*-section fewer times (once per minute; see Methods), which effectively eliminated APP+ photobleaching and allowed us to track puncta over 6 min of continuous electrical stimulation. This duration of 10 Hz stimulation is sufficient to observe the destaining of FFN102 from DA presynaptic terminals, or the destaining of the endocytic dye FM1-43 from excitatory inputs in the striatum.[44] Under these conditions, there was no significant decrease in the number of APP+ puncta (ANOVA, $p > 0.05$, $n = 3$) (Figure 8A). Relative to the number of puncta present at $t = 0$, 94.6 ± 11.8% of puncta were present after 6 min in control unstimulated slices, and 86.7 ± 9.7% of puncta remained after 6 min of 10 Hz electrical stimulation (mean ± SD, $n = 3$). Similarly, there was no statistically significant difference in puncta intensity at the final time point (unstimulated control intensity after 6 min = 89.6 ± 9.2%; 10 Hz stimulation = 91.6 ± 3.1%; mean ± SD, $n = 3$, ANOVA, $p > 0.05$) (Figure 8B). These data show that few if any APP+ puncta underwent complete destaining and that an ensemble of puncta (100s per image) did not undergo significant destaining under conditions of local electrical stimulation. We thus conclude that the binding of APP+ to mitochondria and other cellular compartments within DA synaptic terminals and axonal processes creates a nonreleasable fluorescent background signal that overwhelms the releasable signal and thus limits the dynamic range of the APP+ destaining measurement.

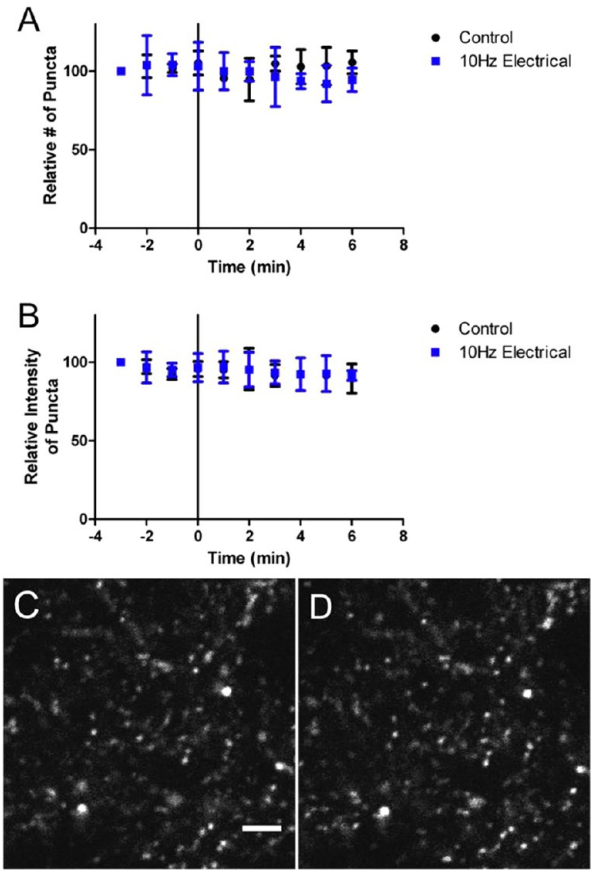


Figure 8. Effect of local 10 Hz electrical stimulation on the number and intensity of stuctures stained by APP+ over time in the dorsal straitum. Stimulation starts at the time point 0 and continues for 6 min, during which time no significant change in (A) relative number of puncta or (B) relative mean punctate intensity could be detected. 10 μm thick *z*-stacks were imaged at each time point to correct for changes in the *z*-plane that might be occurring over time. These stacks were imaged at 1 min intervals to minimize photobleaching of APP+. Included are representative images before (C) and after (D) 6 min application of 10 Hz electrical stimulation.

DISCUSSION

The discovery of MPP+ as a selective dopaminergic toxin followed a report of a young healthy chemistry graduate student who developed chronic parkinsonism after self-administering a homemade batch of the synthetic opioid 1-methyl-4-phenyl-4-propionoxypiperidine (MPPP), which contained the synthetic impurity 1-methyl-4-phenyl-1,2,3,6-tetrahydropyridine (MPTP), resulting from a haphazard synthetic shortcut.[45] On the basis of subsequent investigations, a mechanistic model of MPTP toxicity was proposed. MPTP readily crosses the blood-brain barrier; in the brain it is oxidized by monoamine oxidase-B (MAO-B) to MPP+, which accumulates in DA neurons via uptake by DAT. Inside dopamine neurons, MPP+ binds to mitochondria, an effect driven by the electrochemical gradient across the inner mitochondrial membrane, and inhibits mitochondrial respiration, which eventually leads to cell death.[15,22] It is not fully understood why the SN DA neurons are particularly vulnerable to MPP+ induced cell death, in comparison to the VTA DA neurons, as well as NE and 5HT neurons; however, expression levels of VMAT2 in these cells may be one of the contributing factors.[20,46,47]

MPP+ is a VMAT substrate; inhibition of VMAT2 has been shown to increase neuronal toxicity,[20] while VMAT2 expression protects cells from toxic effects of MPP+ by sequestering the toxin into synaptic vesicles and other VMAT2-expressing acidic organelles.[21,48] Consistent with being a substrate for both DAT and VMAT2, MPP+ was reported to be taken up by presynaptic terminals in the striatum in a DAT-dependent manner and released by perfusion of tissue slices with KCl.[23] Further, the fluorescent analogues of MPP+, ASP+ and APP+, were shown to act as substrates for DAT and other monoamine transporters.[24−26,32,33] These observations therefore suggested that a fluorescent analogue of MPP+ might function as an FFN and provided the rationale for the present study.

APP+ is a close structural analogue of MPP+ that is sufficiently bright for fluorescence microscopy applications.[33] It fluoresces in hydrophobic media but is largely quenched in aqueous environments as discussed above. APP+ is a DAT, NET, and SERT substrate as demonstrated in cell lines transfected with rat or human monoamine transporters and thus provides a useful reporter substrate for these transporters.[32,33] As recently described, APP+ enabled examination of endogenously expressed SERT in platelets and lymphocytes,[38] as well as in an immortalized serotonergic neural cell line.[37]

In the present study, we examined APP+ in acute brain tissue and found that it labeled catecholamine neuronal somata in the midbrain (SN/VTA and LC) as well as dopaminergic axonal processes and presynaptic terminals in the dorsal striatum. Sufficient labeling was accomplished in the dorsal striatum by perfusion of the coronal slice with a low concentration of APP+ (100 nM), which may be ascribed to high expression and

dx.doi.org/10.1021/cn400038u | ACS Chem. Neurosci. XXXX, XXX, XXX−XXX

activity of DAT in this brain region. Indeed, inhibition of DAT with nomifensine afforded a dramatically different staining pattern with a smaller number of puncta (2.3-fold) and greater relative proportion of large punctate structures (>2 μm). Although the inhibition experiment in the dorsal striatum supports the role of DAT in the uptake of APP+ and formation of the fine punctate staining pattern (which is similar to that of TH-GFP and FFN102 signal), it also suggests the presence of other transporter systems capable of transporting APP+ into different cellular structures. Consistent with this are observations in the midbrain (SN/VTA and LC) where, in addition to cell bodies of catecholamine neurons, other structures were labeled throughout the tissue surrounding the neurons. The staining of these unidentified punctate structures was not inhibited by nomifensine and was also present in areas that do not contain catecholamine neurons. It was reported that the endocytic dye FM4-64, a pyridinium analogue of considerably larger size than APP+, is taken up by cortical astrocytes via store-operated Ca^{2+} entry (SOCE) channels.[49] It was also suggested that background staining in brain slice observed with FM4-64 might be due to astrocytic uptake occurring via the SOCE channels. Organic cation transporters such as OCT3, which are widely expressed in the brain and have been shown to transport MPP+,[50,51] may also contribute to extra-catecholaminergic staining by APP+. Additionally, the related pyridinium ASP+ has been used to label implanted glioma cells in mouse brain slices, as OCT3 expression is high in glioma cells.[52] Finally, APP+ is also a substrate for SERT,[32,33] so it is likely that serotonergic structures are labeled.

Although the unidentified punctate staining obscures the dendritic structures, APP+ may serve as a useful marker of catecholamine neuronal cell bodies and as a fluorescent probe for examination of DAT/NET function in acute ex vivo tissue preparations. APP+ may also be used as a marker for DA axonal processes and presynaptic terminals in the dorsal striatum (~75−80% colocalization with TH-GFP and FFN102).

We also examined APP+ label in the dorsal striatum under conditions that induce depolarization and exocytotic neurotransmitter release. Application of a high concentration of KCl led to a small but significant degree of destaining (<15% compared to control), in contrast to a nearly complete destaining of FFN102 under the same conditions.[11] Using 10 Hz local electrical stimulation that more closely mimics physiological conditions, we observed no significant presynaptic terminal destaining of APP+. We were unable to detect APP+ signal in the extracellular space (i.e., released APP+) via two-photon microscopy imaging under any condition, consistent with fluorescent quenching of APP+ in the polar, aqueous extracellular environment. This contrasts with the recently developed probe FFN102, which was designed to produce increased fluorescence when released to the extracellular space from acidic synaptic vesicles.[11]

These results indicate that only a small portion of the APP+ fluorescence signal originates from the releasable synaptic vesicular pool, while the majority of the APP+ signal is derived from an intracellular mixture of labeled nonexocytotic compartments and cellular structures including mitochondria. Our findings are similar to those obtained with the antihypotensive agent amezinium (4-amino-6-methoxy-1-phenyl-pyridazinium salt) reported by others.[53] This pyridinium analogue of similar molecular size and shape to APP+ was taken up by noradrenergic terminals via NET in the rat occipital cortex, which receives noradrenergic inputs from LC; however, only ~1% of the total [^{3}H]-amezinium tissue content was released upon electrical stimulation of brain slices. These results clearly indicate that only a small portion of amezinium is taken up by synaptic vesicles and thus releasable by exocytosis.

Our data indicate that APP+ is not a promising candidate for use in kinetic measurements of individual presynaptic terminals and thus is not a promising lead for development of catecholaminergic FFNs. However, the structural and behavioral similarities of APP+ to the mitochondrial potential probe DASPMI[30,54] may facilitate the selective study of mitochondrial function in catecholamine neurons in brain tissue.

CONCLUSIONS

In this study, we investigated the staining characteristics of the fluorescent pyridinium dye APP+ in selected areas of the acute mouse brain tissue. As a DAT and NET substrate, APP+ labels catecholamine neuronal cell bodies with high selectivity in the relevant midbrain regions, namely, SN/VTA and LC. Although dendritic processes are largely obscured by punctate staining that is DAT or NET-independent, the somata of catecholamine neurons can readily be identified. Thus APP+ could be used as a maker of catecholamine neurons in the absence of additional fluorescent markers, such as the GFP signal in TH-GFP mice. APP+ also enables examination of DAT and NET function in these neurons in the native context of ex vivo brain tissue sections. Since APP+ labels mitochondria inside the cells, it may be envisioned that if the mitochondrial accumulation of the dye is dependent on the mitochondrial membrane potential, APP+ may serve as a catecholamine-neuron selective reporter of mitochondrial function.

We also showed that APP+ might serve as an approximate marker of dopaminergic axonal processes and presynaptic terminals in the dorsal striatum (75−80% colocalization with GFP in TH-GFP mice and FFN102 in wild type mice) that is largely stable to exocytotic conditions. It was found that only a small degree of signal destaining occurs (<15%) when depolarization is induced by KCl or electrical stimulation. This can be attributed to low uptake of APP+ by synaptic vesicles and (or) quenching of the fluorescence signal in the vesicular lumen. Therefore, APP+ is not readily adaptable for quantitative imaging of exocytosis and neurotransmitter secretion and thus is not well suited for the development of new FFNs.

METHODS

Epifluorescence Microscopy in hDAT-EM4 and EM4 Cells. An EM4 cell line stably expressing hDAT (hDAT-EM4) and an empty-vector transfected EM4 cell line to serve as a control were kindly provided by Drs. Jonathan Javitch and Mark Sonders of the Department of Psychiatry at Columbia University Medical Center. Cells were grown in DMEM + glutamax (Invitrogen #10569) with 10% fetal bovine serum (FBS) (Atlanta Biologicals), 100 U/mL penicillin (Invitrogen), and 100 μg/mL streptomycin (Invitrogen). For fluorescence microscopy experiments, cells were plated on poly-D-lysine (Sigma-Aldrich, 0.1 mg/mL) coated six-well plates (Falcon) at a density of 100 000 cells/well and were incubated until confluence (4 days at 37 °C in a humidified atmosphere containing 5% CO_2). The medium was then removed by aspiration, and wells were carefully washed with PBS (2 mL/well). Cells were then treated with 900 μL of experimental medium (DMEM minus phenol red containing 25 mM HEPES (Invitrogen) with 1% FBS (Atlanta Biologicals)) for 3 h. To investigate intracellular localization of APP+, solutions of APP+ (20 μM), Mitotracker Deep Red (200 nM) (Invitrogen), or a mixture of both in 100 μL of experimental medium (all prepared from stock

solutions in DMSO) were added to wells for final concentrations of 2 μM APP+ and 20 nM mitotracker in 1 mL of experimental medium. After incubating at 37 °C for 10 min, images were taken using a Leica DMI 4000B inverted epifluorescence microscope equipped with a Leica DFC 360 FX digital camera controlled through Leica LAS AF 6000E software. Bright field and fluorescence images were acquired sequentially (BF acquisition time = 37 ms). Fluorescence images were acquired using filter cubes (APP+, ex = 440 ± 25 nm, em = 550 ± 25 nm, 500 ms acquisition time; Mitotracker Deep Red, ex = 580 ± 20 nm, em = 660 ± 25 nm, 500 ms acquisition time). Using these filters, no crosstalk was observed between fluorophores. All images of each fluorophore were adjusted to the same brightness and contrast level using ImageJ (National Institutes of Health).

Mouse Coronal Brain Slice Preparation. All animals used for slice preparation for striatal experiments were 2−4 month old male C57BL/6 mice obtained from the Jackson Laboratory (Bar Harbor, ME). The same mice at 20−30 days postnatal were used for midbrain experiments. All animal protocols were approved by the IACUC of Columbia University. For striatal slice preparation, mice were decapitated and acute 300 μm thick coronal slices were cut on a vibratome at 4 °C and allowed to recover for 1 h before use at room temperature in oxygenated (95% O_2, 5% CO_2) artificial cerebrospinal fluid (ACSF) containing (in mM): 125 NaCl, 2.5 KCl, 26 $NaHCO_3$, 0.3 KH_2PO_4, 2.4 $CaCl_2$, 1.3 $MgSO_4$, 0.8 NaH_2PO_4, 10 glucose (pH 7.2−7.4, 292−296 mOsm/L).

Application and Imaging of APP+. Slices were transferred to an imaging chamber (QE-1, Warner Instruments, Hamden, CT), held in place with a platinum wire and nylon custom-made holder,[44] and superfused (1−3 mL/min) with oxygenated ACSF. APP+ (100 nM in ACSF) was loaded into the slice during a 15 min perfusion at room temperature in oxygenated ACSF. Slices were allowed to wash in the perfusion chamber for 10 min before imaging. Nomifensine treated slices were incubated with 1 μM nomifensine for 15 min, before being added to the imaging chamber, after which the slices were coincubated with 100 nM APP+ and 1 μM nomifensine.

Fluorescent structures were visualized at >25 μm depth in the slice using a Prairie Ultima Multiphoton Microscopy System (Prairie Technologies, Middleton, WI) with a titanium-sapphire Chameleon laser (Coherent) equipped with a 60 × 0.9 NA water immersion objective. APP+ was excited at 810 nm and imaged using an emission range of 440−500 nm. For striatal slices, images were captured in 16-bit 37.3 × 37.3 μm^2 field of view (FOV) at 512 × 512 pixel resolution and a dwell time of 10 μs/pixel using Prairie View software.

Imaging Catecholamine Neuronal Cell Bodies: Colocalization of APP+ and GFP in TH-GFP Mice. Midbrain coronal slices were collected from TH-GFP mice 20 − 25 days old due to a reported downregulation of NET on the surface of noradrenergic cell bodies in the LC after 30 days postnatal.[41,42] Dopaminergic cell bodies in the midbrain, from both the substantia nigra and ventral tegmental areas, and noradrenergic cell bodies from the locus coeruleus as determined by GFP fluorescence, were incubated using a higher 500 nM APP+ for 30 min. The midbrain slice was then washed with ACSF for 10 min prior to imaging. In order to minimize crosstalk between fluorophores, APP+ was detected using an excitation of 800 nm and an emission range of 435−485 nm, and GFP was detected using an excitation of 950 nm and an emission range of 500−550 nm (see the Supporting Information for relevant spectral information). To ensure that no shift in z occurs while the laser switches between wavelengths, a second APP+ image was collected at the end and compared to the first. Images were captured in 16-bit 112 × 112 μm FOV at 1024 × 1024 pixel resolution and a dwell time of 10 μs/pixel using Prairie View software.

Imaging Dopaminergic Axonal Processes in the Dorsal Striatum: Colocalization with TH-GFP. After 100 nM probe incubation, striatal slices of TH-GFP animals were imaged with the same acquisition protocol as midbrain experiments described above, in order to minimize signal crosstalk between fluorophores. APP+ was detected using an excitation wavelength of 800 nm and an emission of 435−485 nm. GFP was detected using an excitation of 950 nm and an emission of 500−550 nm. To ensure that no shift in z occurs while tuning the laser between wavelengths, a second APP+ image was collected after GFP acquisition and compared to the first. It is also important to check for any crosstalk between the two fluorophores. Control experiments showed a lack of GFP signal using APP+ acquisition parameters, however approximately 10% of APP+ puncta signal were apparent in the 500−550 nm channel when using GFP acquisition parameters (see the Supporting Information for control images). To assess whether APP+ signal was localized to dopaminergic neurons, we also measured colocalization of APP+ with the previously established dopaminergic marker FFN102, which has an excitation/emission spectrum that is more readily separated from APP+.

Colocalization of APP+ with FFN102. Striatal slices were preincubated with 10 μM FFN102 for 30 min and then added to the imaging chamber where 100 nM APP+ was perfused over the slices for 15 min. After a 5 min wash, APP+ was detected at an excitation of 810 nm and an emission of 570−640 nm. FFN102 was detected using an excitation of 740 nm and an emission of 430−500 nm. To ensure that no shift in z occurs during laser tuning between wavelengths, a second APP+ image was collected at the end and compared to the first. We confirmed a lack of signal in the APP+ and FFN102 channels by their alternative fluorophore using control slices incubated in either APP+ or FFN102 (see the Supporting Information for control images).

APP+ Destaining with KCl. For experiments with potassium chloride, 40 mM KCl in ACSF was perfused over the slice. There is significant slice distortion when 40 mM KCl is used, making tracking the same objects over time difficult. For these experiments, 50 μm z-stacks comprising 10 images, each image taken at 5 μm intervals, were collected every 1 min. The start of the z-stack would begin above the surface of the slice and continue down past the 25 μm depth previously used. From this data, it was possible to determine which z-plane contained the surface of the slice, and then the slice that was ∼25 μm from the surface was used for quantification.

Electrical Stimulation of APP+ Loaded Brain Slice. For electrical experiments, the AMPA and NMDA receptor inhibitors NBQX (10 μM) and AP-5 (50 μM) were included during the perfusion wash and throughout the rest of the experiment. To compensate for shifts in the z-plane during time course imaging, z-stacks were acquired. For initial experiments previously optimized for FFN imaging, 5 μm z-stacks comprising five images, each image taken at 1 μm intervals, were collected every 15 s, over a total of 9 min (3 min with no stimulation to monitor baseline, followed by 6 min of electrical stimulation). However, under these conditions APP+ was photobleaching; each z-plane was nominally excited for a total of 105 s over the course of the experiment, although this time was likely considerably longer due to the poor z-resolution of excitation. The extent to which APP+ undergoes photobleaching was determined by collecting images using the standard protocol (see above), but without electrical stimulation, and comparing the results to images collected only at the first and last time point (a total of 9 min interval). To reduce photobleaching and to more readily facilitate the tracking of puncta throughout the experiment, 10 μm z-stacks comprising 10 images were collected every 1 min over a total of 9 min (3 min with no stimulation to monitor baseline, followed by 6 min of electrical stimulation). At the start of electrical stimulation, a 10 Hz stimulation train (each pulse 200 ms × 130−150 mA) was applied locally to the dorsal striatum for 6 min. Stimulation was locally applied via an Iso-Flex stimulus isolator triggered by a Master-8 pulse generator (AMPI, Jerusalem, Israel), using stainless steel bipolar electrodes.

Data Analysis. Quantification of colocalization of fluorophores was determined using Volocity image analysis software version 4.4 (Improvision, PerkinElmer). Fluorescent puncta were identified by defining a threshold of intensity as well as size and shape parameters (see Volocity user guide for a more detailed description of the object identification tasks; http://cellularimaging.perkinelmer.com/pdfs/manuals/VolocityUserGuide.pdf). After an automatic selection of the objects by the program, a manual inspection was performed, where each object was visually inspected to confirm its validity. Selected objects that did not conform to a certain number of properties (appropriate size, rounded shape, and well-delimited boundaries) were discarded.

We determined object colocalization between APP+ and either FFN102 or GFP channels using Volocity's "Measure Object Colocalization" task that calculates a colocalization coefficient, which indicates the fraction of the signal above threshold in one channel that exists as colocalized with a second channel.[55] Colocalization coefficients ranging from 0 (none of the signal above threshold in that channel exists as colocalized with the other channel) to 1 (all of the signal above threshold in that channel exists as colocalized with the other channel) for each of the selected objects were then obtained. A colocalization coefficient of 0.5 or higher was considered to be indicative of colocalization. Results are expressed as percentage of APP + objects that colocalize with FFN102 or GFP ± SD, and were calculated from at least three independent experiments (at least two slices per experiment, ~150 puncta per slice).

For coronal midbrain slices, cells were considered positive for either fluorophore if their mean fluorescence intensity was above 2× SD of the mean background fluorescence intensity, which was determined in an area devoid of fluorescent puncta/cells. The number of cells was manually counted in images from at least three different positions per area from three different animals.

Volocity was also used to identify puncta with and without nomifensine, and at each time point during incubation with and without KCl. For KCl experiments, mean intensity values of selected objects at each time point were normalized to the time point just before KCl stimulation and then plotted as a function of time using GraphPad Prism 4. The final changes of puncta fluorescence and puncta number at each time point were then compared to an untreated control using an unpaired two-tailed t test to determine statistical significance. Data presented as averages ± SD from three independent experiments (approximately two slices per condition per experiment).

For electrical destaining experiments, MacBiophotonics ImageJ was used for analysis, as Volocity cannot correct for shifts in the z plane. An in-house written macro was used to correct for movement in the z dimension throughout the time course. Registration in $x-y$ was achieved using the PoorMan3DReg plugin (written by Michael Liebling, University of California, Santa Barbara, as a modification of Philippe Thévenaz's, École Polytechnique Fédérale de Lausanne, Switzerland, plug-in StackReg). The Multiple Thresholds plug-in (created by Damon Poburko, Simon Fraser University, Burnaby, BC, Canada) was then used for fluorescent puncta identification at each time point. Upon visual inspection, objects that did not conform to defined properties (appropriate size, rounded shape, and well delimited boundaries) were discarded, as well as puncta that moved significantly out of the object mask during the time frame analyzed. The mean intensity and number of puncta at each time point were then normalized to the time point before stimulation and plotted as a function of time using GraphPad Prism 4. The final changes of puncta fluorescence and puncta number after stimulation were then compared using an unpaired two-tailed t test for statistical significance. Data presented as averages ± SD from three independent experiments (two slices per condition per experiment).

■ ASSOCIATED CONTENT

Supporting Information

Synthetic procedures for APP+, protocols for photophysical methods, discussion of APP/GFP signal crosstalk, and images from additional control studies. This material is available free of charge via the Internet at http://pubs.acs.org.

■ AUTHOR INFORMATION

Corresponding Author

*(D. Sulzer) Mailing address: Columbia University Medical Center, Black 308, 650 W 168th St, New York, NY 10032. E-mail: ds43@columbia.edu. (D. Sames) Mailing address: Department of Chemistry, Columbia University, 3000 Broadway, MC3101, New York, NY 10027. E-mail: ds584@columbia.edu.

Author Contributions

All authors have given approval to the final version of the manuscript. R.J.K. and M.D. contributed equally.

Funding

This work was supported by the National Institute of Mental Health (R01MH086545), the G. Harold & Leila Y. Mathers Charitable Foundation, NIDA DA07418 and DA010154, and the Parkinson's Disease Foundation and the JPB Foundation.

Notes

The authors declare no competing financial interest.

■ ACKNOWLEDGMENTS

We thank Dr. Mark Sonders for providing the EM4 and hDAT-EM4 cells used in this study, as well as for helpful discussions. We also thank Dr. Anders Borgkvist for assistance with 2 photon microscopy.

■ ABBREVIATIONS

APP+, 4-(4-dimethylamino)phenyl-1-methylpyridinium; MPP+, 1-methyl-4-phenylpyridinium; FFN, fluorescent false neurotransmitter; DAT, dopamine transporter; NET, norepinephrine transporter; SERT, serotonin transporter; VMAT2, vesicular monoamine transporter 2; DA, dopamine; SN/VTA, substantia nigra/ventral tegmental area; LC, locus coeruleus

■ REFERENCES

(1) Banks, R. W. (1999) Cytological staining methods. In *Modern Techniques in Neuroscience Research* (Windhorst, U., and Johansson, H., Eds.), pp 1−26, Springer-Verlag, Berlin & Heidelberg.

(2) Nimmerjahn, A., Kirchhoff, F., Kerr, J. N., and Helmchen, F. (2004) Sulforhodamine 101 as a specific marker of astroglia in the neocortex *in vivo*. *Nat. Methods 1*, 31−37.

(3) Lee, J.-S., Kim, Y. K., Vendrell, M., and Chang, Y.-T. (2009) Diversity-oriented fluorescence library approach for the discovery of sensors and probes. *Mol. BioSyst. 5*, 411−421.

(4) Haugland, R. P. (2002) *Handbook of Fluorescent Probes and Research Products* (Gregory, J., Ed.), 9th ed., Molecular Probes, Inc., Eugene, OR.

(5) Kawanishi, T., Blank, L. M., Harootunian, A. T., Smith, M. T., and Tsien, R. Y. (1989) Ca^{2+} Oscillations Induced by Hormonal Stimulation of Individual Fura-2-loaded Hepatocytes. *J. Biol. Chem. 264*, 12859−12866.

(6) Tsien, R. Y. (1980) New calcium indicators and buffers with high selectivity against magnesium and protons: Design, synthesis, and properties of prototype structures. *Biochemistry 19*, 2396−2404.

(7) Peterka, D., Takahashi, H., and Yuste, R. (2011) Imaging Voltage in Neurons. *Neuron 69*, 9−21.

(8) Gaffield, M. A., and Betz, W. J. (2006) Imaging synaptic vesicle exocytosis and endocytosis with FM dyes. *Nat. Protoc. 1*, 2916−2921.

(9) Sames, D., Dunn, M., Krapowicz, R. J., Jr., and Sulzer, D. (2013) Visualizing Neurotransmitter Secretion at Individual Synapses. *ACS Chem. Neurosci.* DOI: 10.1021/cn4000956.

(10) Gubernator, N. G., Zhang, H., Staal, R. G. W., Mosharov, E. V., Pereira, D. B., Yue, M., Balsanek, V., Vadola, P. A., Mukherjee, B., Edwards, R. H., Sulzer, D., and Sames, D. (2009) Fluorescent False Neurotransmitters Visualize Dopamine Release from Individual Presynaptic Terminals. *Science 324*, 1441−1444.

(11) Rodriguez, P. C., Pereira, D. B., Borgkvist, A., Wong, M. Y., Barnard, C., Sonders, M. S., Zhang, H., Sames, D., and Sulzer, D. (2013) Fluorescent dopamine tracer resolves individual dopaminergic synapses and their activity in the brain. *Proc. Natl. Acad. Sci. U.S.A. 110*, 870−875.

(12) Wise, R. A. (2004) Dopamine, learning and motivation. *Nat. Rev. Neurosci. 5*, 483−494.

(13) Arbuthnott, G. W., and Wickens, J. (2007) Space, time and dopamine. *Trends Neurosci. 30*, 62−69.

(14) Sotnikova, T. D., Beaulieu, J.-M., Gainetdinov, R. R., and Caron, M. G. (2006) Molecular biology, pharmacology and functional role of the plasma membrane dopamine transporter. *CNS Neurol. Disord.: Drug Targets 5*, 45−56.
(15) Javitch, J. A., D'Amato, R. J., Strittmatter, S. M., and Snyder, S. H. (1985) Parkinsonism-inducing neurotoxin, *N*-methyl-4-phenyl-1,2,3,6-tetrahydropyridine: Uptake of metabolite *N*-methyl-4-phenylpyridine by dopamine neurons explains selective toxicity. *Proc. Natl. Acad. Sci. U.S.A. 82*, 2173−2177.
(16) Gainetdinov, R. R., Fumagalli, F., Jones, S. R., and Caron, M. G. (1997) Dopamine transporter is required for in vivo MPTP neurotoxicity: evidence from mice lacking the transporter. *J. Neurochem. 69*, 1322−1325.
(17) Buck, K. J., and Amara, S. G. (1994) Chimeric dopamine-norepinephrine transporters delineate structural domains influencing selectivity for catecholamines and 1-methyl-4-phenylpyridinium. *Proc. Natl. Acad. Sci. U.S.A. 91*, 12584−12588.
(18) Wall, S. C., Gu, H., and Rudnick, G. (1995) Biogenic Amine Flux Mediated by Cloned Transporters Stably Expressed in Cultured Cell Lines: Amphetamine Specificity for Inhibition and Efflux. *Mol. Pharmacol. 47*, 544−550.
(19) Yelin, R., and Schuldiner, S. (1995) The pharmacological profile of the vesicular monoamine transporter resembles that of multidrug transporters. *FEBS Lett. 337*, 201−207.
(20) Staal, R. G., and Sonsalla, P. K. (2000) Inhibition of Brain Vesicular Monoamine Transporter (VMAT2) Enhances 1-Methyl-4-phenylpyridinium Neurotoxicity In Vivo in Rat Striata. *J. Pharmacol. Exp. Ther. 293*, 336−342.
(21) Liu, Y., Peter, D., Roghani, A., Schuldiner, S., Privé, G. G., Eisenberg, D., Brecha, N., and Edwards, R. H. (1992) A cDNA That Suppresses MPP+ Toxicity Encodes a Vesicular Amine Transporter. *Cell 70*, 539−551.
(22) Singer, T. P., Ramsay, R. R., McKeown, K., Trevor, A., and Castagnoli, N. E. (1988) Mechanism of the Neurotoxicity of 1-Methyl-4-phenylpyridinium (MPP+), the Toxic Bioactivation Product of 1-Methyl-4-phenyl-1,2,3,6-tetrahydropyridine (MPTP). *Toxicology 49*, 17−23.
(23) Keller, H. H., and da Prada, M. (1985) Evidence for the release of 1-methyl-4-phenylpyridinium (MPP+) from rat striatal neurons in vitro. *Eur. J. Pharmacol. 119*, 247−250.
(24) Schwartz, J. W., Blakely, R. D., and DeFelice, L. J. (2003) Binding and Transport in Norepinephrine Transporters. *J. Biol. Chem. 278*, 9768−9777.
(25) Schwartz, J. W., Novarino, G., Piston, D. W., and DeFelice, L. J. (2005) Substrate Binding Stoichiometry and Kinetics of the Norepinephrine Transporter. *J. Biol. Chem. 280*, 19177−19184.
(26) Brown, A. S., Bernal, L.-M., Micotto, T. L., Smith, E. L., and Wilson, J. N. (2011) Fluorescent neuroactive probes based on stilbazolium dyes. *Org. Biomol. Chem. 9*, 2142−2148.
(27) Kolomoitsev, P. R. (1962) Antibacterial properties of some N-substituted pyridine derivatives. *Mikrobiol. Z. 24*, 23−27.
(28) Hutchings, M. G. (1984) Structure-colour relationships of some new *N*-arylpyridinium hemicyanine dyes. *Tetrahedron 40*, 2061−2068.
(29) Fromherz, P., and Heilemann, A. (1992) Twisted Internal Charge Transfer in (Aminophenyl)pyridinium. *J. Phys. Chem. 96*, 6864−6866.
(30) Bereiter-Hahn, J. (1976) Dimethylaminostyrylmethylpyridiniumiodine (daspmi) as a fluorescent probe for mitochondria in situ. *Biochim. Biophys. Acta 423*, 1−14.
(31) Betz, W. J., Mao, F., and Bewick, G. S. (1992) Activity-dependent fluorescent staining and destaining of living vertebrate motor nerve terminals. *J. Neurosci. 12*, 363−375.
(32) Blakely, R. D., Mason, J. N., Tomlinson, I. D., and Rosenthal, S. J. Fluorescent Substrates for Neurotransmitter Transporters. U.S. Patent 7,947,255, May 24, 2011.
(33) Solìs, E., Jr., Zdravkovic, I., Tomlinson, I. D., Noskov, S. Y., Rosenthal, S. J., and DeFelice, L. J. (2012) 4-(4-(Dimethylamino)-phenyl-1-methylpyridinium (APP^+) is a Fluorescent Substrate for the Human Serotonin Transporter. *J. Biol. Chem. 287*, 8852−8863.
(34) Parker, L. K., Shanks, J. A., Kennard, J. A., and Brain, K. L. (2010) Dynamic monitoring of NET activity in mature murine sympathetic terminals using a fluorescent substrate. *Br. J. Pharmacol. 159*, 797−807.
(35) Jørgensen, S., Nielson, E. Ø., Peters, D., and Dyhring, T. (2008) Validation of a fluorescence-based high-throughput assay for the measurement of neurotransmitter transporter uptake activity. *J. Neurosci. Methods 169*, 168−176.
(36) Bernstein, A. I., Stout, K. A., and Miller, G. W. (2012) A fluorescent-based assay for live cell, spatially resolved assessment of vesicular monoamine transporter 2-mediated neurotransmitter transport. *J. Neurosci. Methods 209*, 357−366.
(37) Chang, J. C., Tomlinson, I. D., Warnement, M. R., Ustione, A., Carneiro, A. M., Piston, D. W., Blakely, R. D., and Rosenthal, S. J. (2012) Single Molecule Analysis of Serotonin Transporter Regulation Using Antagonist-Conjugated Quantum Dots Reveals Restricted, p38 MAPK-Dependent Mobilization Underlying Uptake Activation. *J. Neurosci. 32*, 8919−8929.
(38) Biekmann, B. S., Tomlinson, I. D., Rosenthal, S. J., and Andrews, A. M. (2012) Serotonin Uptake is Largely Mediated by Platelets versus Lymphocytes in Peripheral Blood Cells. *ACS Chem. Neurosci. 4*, 161−170.
(39) Matsushita, N., Okada, H., Yasoshima, Y., Takahashi, K., Kazutoshi, K., and Kobayashi, K. (2002) Dynamics of tyrosine hydroxylase promoter activity during midbrain dopaminergic neuron development. *J. Neurochem. 82*, 295−304.
(40) Borgden, R. N., Heel, R. C., Speight, T. M., and Avery, G. S. (1979) Nomifensine: A review of its pharmacological properties and therapeutic efficacy in depressive illness. *Drugs 18*, 1−24.
(41) Sanders, J. D., Happe, H. K., Bylund, D. B., and Murrin, L. C. (2005) Development of the Norepinephrine Transporter in the Rat CNS. *Neuroscience 130*, 107−117.
(42) Murrin, L. C., Sanders, J. D., and Bylund, D. B. (2007) Comparison of the maturation of the adrenergic and serotonergic neurotransmitter systems in the brain: Implications for differential drug effects on juveniles and adults. *Biochem. Pharmacol. 73*, 1225−1236.
(43) Bamford, N. S., Zhang, H., Schmitz, Y., Wu, N. P., Cepeda, C., Levine, M. S., Schmauss, C., Zakharenko, S. S., Zablow, L., and Sulzer, D. (2004) Heterosynaptic dopamine neurotransmission selects sets of corticostriatal terminals. *Neuron 42*, 653−663.
(44) Wong, M. Y., Sulzer, D., and Bamford, N. S. (2011) Imaging presynaptic exocytosis in corticostriatal slices. *Methods Mol. Biol. 793*, 363−376.
(45) Davis, G. C., Williams, A. C., Markey, S. P., Ebert, M. H., Caine, E. D., Reichert, C. M., and Kopin, I. J. (1979) Chronic Parkinsonism Secondary to Intravenous Injection of Meperidine Analogues. *Psychiatry Res. 1*, 249−254.
(46) Nirenberg, M. J., Chan, J., Liu, Y., Edwards, R. H., and Pickel, V. M. (1996) Ultrastructural Localization of the Vesicular Monoamine-Transporter-2 in Midbrain Dopaminergic Neurons: Potential Sites for Somatodendritic Storage and Release of Dopamine. *J. Neurosci. 16*, 4135−4145.
(47) Nirenberg, M. J., Chan, J., Liu, Y., Edwards, R. H., and Pickel, V. M. (1997) Vesicular monoamine transporter-2: immunogold localization in striatal axons and terminals. *Synapse 26*, 194−198.
(48) Adam, Y., Edwards, R. H., and Schuldiner, S. (2008) Expression and function of the rat vesicular monoamine transporter 2. *Am. J. Physiol.: Cell Physiol. 294*, C1004−C1011.
(49) Li, D., Hérault, K., Oheim, M., and Ropert, N. (2009) FM dyes enter via a store-operated calcium channel and modify calcium signaling of cultured astrocytes. *Proc. Natl. Acad. Sci. U.S.A. 106*, 21960−21965.
(50) Wu, X., Kekuda, R., Huang, W., Fei, Y. J., Leibach, F. H., Chen, J., Conway, S. J., and Ganapathy, V. (1998) Identity of the Organic Cation Transporter OCT3 as the Extraneuronal Monoamine Transporter ($uptake_2$) and Evidence for the Expression of the Transporter in the Brain. *J. Biol. Chem. 273*, 32776−32786.

(51) Duan, H., and Wang, J. (2010) Selective Transport of Monoamine Neurotransmitters by Human Plasma Membrane Monoamine Transporter and Organic Cation Transporter 3. *J Pharmacol. Exp. Ther. 335*, 743−753.
(52) Kucheryavykh, L. Y., Kucheryavykh, Y. V., Rolón-Reyes, K., Skatchkov, S. N., Eaton, M. J., Cubano, L. A., and Inyushin, M. (2012) Visualization of implanted GL261 glioma cells in living mouse brain slices using fluorescent 4-(4-(dimethylamino)-styryl)-*N*-methylpyridinium iodide (ASP+). *Biotechniques 53*, 305−309.
(53) Starke, K. (1983) Amezinium: A novel pattern of effects on the sympathetic nervous system. *Trends. Pharmacol. Sci. 4*, 269−272.
(54) Ramadass, R., and Bereiter-Hahn, J. (2008) How DASPMI reveals mitochondrial membrane potential: fluorescence decay kinetics and steady-state anisotropy in living cells. *Biophys. J. 95*, 4068−4076.
(55) Manders, E. M. M., Verbeek, F. J., and Aten, J. A. (1993) Measurement of co-localization of objects in dual-colour confocal images. *J. Microsc. 169*, 375−382.